

Estimation of Blade Structural Properties from Experimental Data

C.L. Bottasso, S. Cacciola, A. Croce*

Dipartimento di Ingegneria Aerospaziale, Politecnico di Milano, Milano, Italy

Scientific Report DIA-SR 11-01,
April 2011

Abstract

Wind turbine blades, being realized using composite materials and designed under a number of aero-elastic and manufacturing constraints, often present complex distributions of the stiffness, mass and inertial properties along their spans.

We propose a method whose goal is to estimate such physical parameters so as to match given experimental observations. The procedure can be used to understand the nature of possible discrepancies between designed and manufactured blade, and to provide updated high fidelity mathematical beam models to be used in aero-elastic simulations. The formulation is based on the constrained optimization of a maximum likelihood cost function, and a noisy measurement fusion approach whereby the data of multiple experiments are used simultaneously in the estimation process.

The proposed method is demonstrated first using simulated data, and then in the identification of two real small wind turbine blades.

*Corresponding author, Dipartimento di Ingegneria Aerospaziale, Politecnico di Milano, Milano, Via La Masa 34, 20156 Italy. E-mail: carlo.bottasso@polimi.it; Tel.: +39-02-2399-8315; Fax: +39-02-2399-8334.

Contents

Notation	3
1 Introduction	4
2 Formulation	5
2.1 Maximum likelihood estimation	5
2.2 Model updating including modal and static response data	6
2.3 Model updating by constrained optimization	7
2.4 Definition of model parameters	9
3 Results	10
3.1 Preliminary study using simulated data	10
3.2 Model update of wind turbine blades	12
3.2.1 Blade A	12
3.2.2 Blade B	13
4 Conclusions	22

List of Figures

1 Definition of identification parameters for the preliminary simulation study	10
2 Sketch of saddle used for the loading of blade A	12
3 Static deflections for some loading conditions of blade A	14
4 Blade A: span-wise distributions of properties	15
5 Sketch of saddle used for the loading of blade B	16
6 Laser scanner images of blade and supporting frame	18
7 Computation of translation and rotation of a blade section	19
8 FFT of some blade accelerometers for shock hammer tests	19
9 Static deflections for the loading conditions of blade B	20
10 Blade B: span-wise distributions of properties	21

List of Tables

1 Identified parameters for the preliminary study using simulated data	11
2 Lowest natural frequencies of blade A	13
3 Lowest natural frequencies of blade B	21

Notation

\mathbf{c}	Vector of equality and/or inequality constraints
\mathbf{p}	Vector of unknown parameters
\mathbf{r}	Vector of residuals
\mathbf{s}	Sectional displacement vector
\mathbf{y}	Vector of outputs
\mathbf{z}	Vector of measurements
$\boldsymbol{\psi}$	Sectional rotation vector
\mathbf{G}	Sensitivity of outputs wrt parameters
\mathbf{R}	Error covariance matrix
\mathbf{T}	Sectional rotation tensor
α_i	Scaling parameter for i th blade property
$\alpha_{i_j}^k$	j th nodal value for i th scaling parameter on k th segment
$\boldsymbol{\phi}$	Mode shape
ω	Natural frequency
π_i	i th blade property
J	Cost function
L	Blade length
M	Blade mass
m	Number of outputs
m_M	Number of modal outputs
m_S	Number of static deflection outputs
N	Number of observations
n	Number of unknown parameters
N_M	Number of modes
N_S	Number of load cases
N_{mark}	Number of sectional markers
N_{nodes}^k	Number of nodes on segment k
N_{prop}	Number of unknown properties
N_{segm}	Number of segments
s	Span-wise coordinate, $s \in [0, L]$
$(\cdot)^*$	Optimal quantity
$(\cdot)^0$	Initial (baseline) quantity
$(\cdot)^k$	Quantity pertaining to k th segment
$(\cdot)^T$	Transpose
$(\cdot)_M$	Quantity associated with modal measurements
$(\cdot)_S$	Quantity associated with static deflection measurements
(\cdot)	True value
$(\hat{\cdot})$	Scaled quantity

1 Introduction

The formulation of beam elements has received considerable attention in the literature. Some complex applications, such as anisotropic helicopter and wind turbine rotor blades, are solved using geometrically exact formulations with fully-populated stiffness properties obtained by the use of sectional analysis theories (see for example Ref. [1] and references therein). In turn, these models are used for performing simulations in all necessary operating conditions using a plethora of multi-disciplinary aero-servo-elastic modeling tools, with the purpose of estimating loads, stability boundaries, vibration levels and other quantities of interest, as well as for the tuning and verification of control laws.

The rotor blades of modern wind turbines, being realized using composite materials and designed under a number of aero-elastic and manufacturing constraints, are typically characterized by complex distributions of the stiffness, mass and inertial properties along their spans. Often, manufactured blades present characteristics that differ in a non negligible way from their theoretical design values. The reasons for this are numerous, and include manufacturing processes, uncertain material properties, modeling approximations, etc.

To understand the nature of the discrepancies between designed and manufactured blades, and to provide updated mathematical models that exhibit the best possible fidelity to the reality, it is useful to devise procedures that provide estimates of the physical parameters of the blade on the basis of experimental measures obtainable on the manufactured items.

This paper describes the development of model update procedures [2] applicable to wind turbine blades; this problem is part of the broader task of system identification of wind turbines. The formulation is based on an output error maximum likelihood parameter estimation approach [3, 4, 5]. The free parameters of the estimation problem are represented by the structural and mass characteristics of a beam model of the blade. An ad hoc interpolation scheme is used to keep the number of free parameters to a minimum, while at the same time accounting for the rapidly varying and often discontinuous distributions of physical properties along the span of typical modern wind turbine blades.

The parameter estimation is formulated as a constrained optimization problem, solved using a Sequential Quadratic Programming (SQP) approach [6]. The cost function is formulated in terms of the maximum likelihood function and can account for multiple measurements of given system outputs, which include natural frequencies, mode shapes, static deflections and dynamic responses. The use of the maximum likelihood function allows one to account for the stochastic nature of the problem, due to the presence of noise and uncertainties in the measurements.

The definition of the estimation problem is complemented by a number of equality and/or inequality constraints, including bounds on the physical parameters and the outputs, knowledge of the total mass and of the location of the center of gravity, and the requirement that the updated model improves the Modal Assurance Criterion with respect to the initial baseline model.

Although most published methods in finite element modal updating use exclusively modal data (cf. for example Refs. [7, 8, 9] and references therein), we argue here that one should use all possible sources of information for increasing the reliability of model update procedures. In fact, parameter estimation problems are often ill posed and present multiple solutions; a better observability of the parameters is typically obtained only when enough information is contained in the experimental measurements. To address this issue, the present approach is formulated so that multiple measures can be used simultaneously to yield estimates of the unknown parameters.

The proposed formulation is demonstrated first on simulated data regarding a large wind turbine blade, and then using real experimental measures obtained on two small wind turbine blades.

2 Formulation

2.1 Maximum likelihood estimation

Consider a parametric model $\mathcal{M}(\mathbf{p})$ of a beam, where $\mathbf{p} \in \mathbb{R}^n$ is a vector of parameters (related to stiffness and/or mass properties, as detailed later in §2.4), and define a set of output quantities $\mathbf{y} = \mathbf{h}(\mathbf{p})$, where $\mathbf{y} \in \mathbb{R}^m$. An experimental measurement (observation) of the outputs \mathbf{y} can be expressed as

$$\mathbf{z} = \mathbf{y} + \mathbf{r}, \quad (1)$$

where the error \mathbf{r} is due to measurement and/or modeling errors, the latter generated by modeling approximations and unmodeled or unresolved physical processes in \mathcal{M} with respect to the reality.

Considering a sample of observations $S = \{\mathbf{z}_1, \mathbf{z}_2, \dots, \mathbf{z}_N\}$, the likelihood function is defined as

$$f(S, \mathbf{p}) = \prod_{i=1}^N p(\mathbf{z}_i | \mathbf{p}), \quad (2)$$

where $p(\mathbf{z}_i | \mathbf{p})$ is the probability of the observed variable \mathbf{z}_i given \mathbf{p} . Maximum likelihood estimation seeks to find the most likely vector \mathbf{p} for model \mathcal{M} by maximizing function $f(S, \mathbf{p})$, i.e. it identifies the \mathbf{p} that gives the maximum probability to the measurements. Given the exponential nature of probability densities, the problem is re-formulated as the minimization of the negative logarithm of the likelihood function:

$$\mathbf{p}^* = \arg \min_{\mathbf{p}} J, \quad (3)$$

with $J = -\ln f(S, \mathbf{p})$.

Assuming a normal (Gaussian) distribution with zero mean for the residuals \mathbf{r}_i , $i = 1, N$, and further assuming that the residuals are statistically independent from one another, the likelihood function can be expressed as

$$f(S, \mathbf{p}) = ((2\pi)^m \det \mathbf{R})^{-N/2} \exp\left(-\frac{1}{2} \sum_{i=1}^N \mathbf{r}_i^T \mathbf{R}^{-1} \mathbf{r}_i\right), \quad (4)$$

where

$$E[\mathbf{r}_i \mathbf{r}_j^T] = \mathbf{R} \delta_{ij}, \quad (5)$$

$E[\cdot]$ being the expected value operator, \mathbf{R} the error covariance and δ_{ij} the Kronecker delta symbol. The optimization cost function of problem (3) then becomes

$$J = \frac{mN}{2} \ln 2\pi + \frac{N}{2} \ln \det \mathbf{R} + \frac{1}{2} \sum_{i=1}^N \mathbf{r}_i^T \mathbf{R}^{-1} \mathbf{r}_i. \quad (6)$$

Notice that, for those components of \mathbf{r} due to modeling errors, the assumptions of zero mean and of stochasticity might not be fully satisfied, although they appear to be routinely adopted in practical applications [3].

Following Refs. [3, 4], a robust numerical implementation of problem (3) can be based on a two step sequence, termed Adaptive Covariance Maximum Likelihood (ACML) method:

1. For a given error covariance \mathbf{R} , minimize with respect to the free parameters \mathbf{p} the cost function

$$J = \frac{1}{2} \sum_{i=1}^N \mathbf{r}_i^T \mathbf{R}^{-1} \mathbf{r}_i, \quad (7)$$

which is obtained from Eq. (6) by neglecting all irrelevant constant terms.

2. For a given set of parameters, update the error covariance matrix as (see Ref. [3], Appendix E, for details)

$$\mathbf{R} = \frac{1}{N} \sum_{i=1}^N \mathbf{r}_i \mathbf{r}_i^T. \quad (8)$$

If not enough samples are available to reconstruct an estimate of the error covariance \mathbf{R} , one can further assume the statistical independence of the residual components, so that the covariance becomes

$$\mathbf{R} = \text{diag}(\dots, r_j^2, \dots), \quad j = 1, m. \quad (9)$$

Keeping \mathbf{R} frozen, gives the classical weighted least squares approach.

It can be shown [3, 4] that the Cramér-Rao bounds on the covariance of the estimated parameters \mathbf{p}^* is given by

$$\text{Var}(\bar{\mathbf{p}} - \mathbf{p}^*) \geq \mathbf{F}^{-1}, \quad (10)$$

where $\bar{\mathbf{p}}$ are the true parameters, \mathbf{F} the Fisher information matrix

$$\mathbf{F} = \sum_{i=1}^N \mathbf{G}_i^T \mathbf{R}^{-1} \mathbf{G}_i, \quad (11)$$

and $\mathbf{G}_i = \partial \mathbf{y}_i / \partial \mathbf{p}$ the sensitivity of the observations.

2.2 Model updating including modal and static response data

Typically, multiple experiments can be conducted on a structural member, including measurement of the eigenfrequencies, of the eigenvectors, of static deflections under concentrated or distributed loads, and temporal responses under known excitations. Conceptually, all this data can be profitably used within a single umbrella for conducting a unified model updating procedure, so as to identify the best set of model parameters that fits the available experimental measurements. Notice that this is in reality rarely done in practice. In fact, most model updating procedures usually rely on a single class of experiments, very often limited to modal data acquisition, since for these measurements established experimental procedures are readily available. However, since parameter estimation of complex models is often an ill posed problems for which there are multiple possible solutions, there is a need to accommodate in the estimation process all the experimental data that is available, so as to include all possible sources of information about the observed behavior of the structure.

To address these needs, in this work we develop a maximum likelihood output error formulation that can account for multiple experiments. The output vector is here defined as

$$\mathbf{y} = (\mathbf{y}_M^T, \mathbf{y}_S^T)^T, \quad (12)$$

where \mathbf{y}_M is the set of outputs accounting for modal data (frequencies and, possibly, modal shapes), and \mathbf{y}_S the set of outputs accounting for static deflections.

More precisely, \mathbf{y}_M is defined as

$$\mathbf{y}_M = (\dots, \omega_k, \phi_k^T, \dots)^T, \quad k = 1, N_M, \quad (13)$$

where ω_k is the k th natural modal frequency, ϕ_k its associated modal shape and N_M the number of modes, obtained from the solution of the corresponding eigenvalue problems on model \mathcal{M} :

$$[\omega_k, \phi_k] = \text{eig}(k, \mathbf{p}). \quad (14)$$

If the eigenvectors are not experimentally available, then the set of outputs simply contains the modal frequencies, i.e. $\mathbf{y}_M = (\dots, \omega_k, \dots)^T$. In both cases, we write $\mathbf{y}_M \in \mathbb{R}^{m_M}$, where in the first case $m_M = (1 + N_{\text{nodes}}N_{\text{dc}})N_M$, being N_{nodes} the number of nodes in the FEM model of the blade and N_{dc} the number of displacement components in the modal vector, while $m_M = N_M$ in the second case. The associated maximum likelihood cost function of Eq. (7) is noted J_M .

Consider now the static response of model \mathcal{M} . The vector of structural deflections at the mesh nodes, noted \mathbf{d} , can in general be computed by solving the following system of governing equilibrium equations

$$\mathbf{g}(\mathbf{d}, \mathbf{u}, \mathbf{p}) = \mathbf{0}, \quad (15)$$

where \mathbf{u} is the input (representing either point and/or distributed loads on the structure). Clearly, the governing equations depend on the model parameters \mathbf{p} . For each given loading condition \mathbf{u}_k of the N_S available ones, the corresponding static deflections are noted \mathbf{d}_k and the outputs are defined as

$$\mathbf{y}_{S_k} = \mathbf{h}_S(\mathbf{d}_k), \quad k = 1, N_S, \quad (16)$$

$\mathbf{y}_{S_k} \in \mathbb{R}^{m_y}$, i.e. they are given by some function $\mathbf{h}_S(\cdot)$ of the beam response (for example, they might represent the displacement components at the tip of the beam or at some other given location along the span). Then, the outputs for all loading conditions are gathered together to define the vector of outputs accounting for static deflections, i.e.

$$\mathbf{y}_S = (\dots, \mathbf{y}_{S_k}^T, \dots)^T, \quad k = 1, N_S, \quad (17)$$

where $\mathbf{y}_S \in \mathbb{R}^{m_S}$, $m_S = m_y N_S$. The associated maximum likelihood cost function of Eq. (7) is noted J_S .

2.3 Model updating by constrained optimization

For practical solution of realistic problems, the model parameter estimation given by (3) is reformulated here as the following constrained optimization

$$\min_{\mathbf{p}} J(\mathbf{y}, \mathbf{z}), \quad (18a)$$

$$\text{s.t.}: \mathbf{c}(\mathbf{y}, \mathbf{p}) \leq \mathbf{0}, \quad (18b)$$

$$\mathbf{y}_{\text{lb}} \leq \mathbf{y} \leq \mathbf{y}_{\text{ub}}, \quad (18c)$$

$$\mathbf{p}_{\text{lb}} \leq \mathbf{p} \leq \mathbf{p}_{\text{ub}}, \quad (18d)$$

where the outputs \mathbf{y} were given in (12) and are functions of the unknown parameters \mathbf{p} as detailed in §2.2. Assuming that modal and static measurements are uncorrelated, the maximum likelihood cost J in (18a) can be written as the sum of two terms as

$$J = \frac{1}{m_M} J_M + \frac{1}{m_S} J_S, \quad (19)$$

where J_M and J_S are the maximum likelihood costs expressed by Eq. (7) for, respectively, the modal and static deflection data. Notice that the two cost contributors are scaled by the number

of available measures, m_M and m_S , since the two are typically quite different between each other (e.g., tens of static deflections and only a few eigenfrequencies, as in the examples shown later on).

The formulation of the problem is completed by a number of constraint conditions. Equations (18b) represent possible linear and/or non-linear equality and/or inequality constraints on the outputs and/or the parameters, as detailed further below. Furthermore, Eqs. (18c,18d) specify possible lower and upper bounds on the outputs and the parameters, respectively.

Problem (18) is a Non-Linear Programming Problem (NLP), which can be solved effectively with a number of methods, most notably SQP [6] and Interior Point (IP) [10]. In this work, the former of the two methods was used, with gradients of cost function and constraints computed by finite differences. When eigenvalues and eigenvectors are included in the definition of the problem outputs, their gradients can be computed efficiently by the technique described in Ref. [11], although for other outputs the gradients will in general have to be computed by numerical perturbation means.

As for most optimization problems, it is better to scale all quantities appearing in (18) so as to improve its conditioning. To this end, we define scaled outputs $\hat{\mathbf{y}} = (\dots, \hat{y}_i, \dots)^T$, obtained by dividing each output by its corresponding measure

$$\hat{y}_i = \frac{y_i}{z_i + \delta}, \quad i = 1, m, \quad (20)$$

where $\delta = \|\mathbf{z}\|_2$ is used to avoid divisions by zero; similarly, we define scaled parameters $\hat{\mathbf{p}} = (\dots, \hat{p}_i, \dots)^T$ as

$$\hat{p}_i = \frac{p_i}{p_i^0}, \quad i = 1, m, \quad (21)$$

where \mathbf{p}^0 are values related to the baseline (initial) model; typically, these values are never equal to zero. With these new definitions, the scaled parameter estimation problem becomes

$$\min_{\hat{\mathbf{p}}} J(\hat{\mathbf{y}}, \mathbf{1}), \quad (22a)$$

$$\text{s.t.}: \quad \mathbf{c}(\hat{\mathbf{y}}, \hat{\mathbf{p}}) \leq \mathbf{0}, \quad (22b)$$

$$\hat{\mathbf{y}}_{\text{lb}} \leq \hat{\mathbf{y}} \leq \hat{\mathbf{y}}_{\text{ub}}, \quad (22c)$$

$$\hat{\mathbf{p}}_{\text{lb}} \leq \hat{\mathbf{p}} \leq \hat{\mathbf{p}}_{\text{ub}}, \quad (22d)$$

which in general exhibits superior convergence and robustness when compared to the unscaled problem (18).

Several different constraint types can be appended to the optimization problem by means of Eqs. (22b) so as to account for further sources of knowledge about the solution other than the measurements \mathbf{z} .

For example, when identifying the mass properties of the blade, the measured total mass and center of gravity locations can be enforced as constraints as

$$\mathbf{c} = \begin{pmatrix} 1 - \frac{1}{M} \int_0^L m(s) ds \\ 1 - \frac{1}{s_G} \int_0^L m(s)s ds \end{pmatrix} = \mathbf{0}, \quad (23)$$

where M is the measured total blade mass, $m(s) = m(\mathbf{p}(s))$ is the mass per unit span, $s \in [0, L]$ is a coordinate measured along the beam reference line, being L the beam length, and s_G the

center of gravity location along the span. Notice that here again the equations were written in non-dimensional form for scaling reasons.

To ensure that the eigenvectors computed on the updated model improve the metric quality measure provided by the Modal Assurance Criterion (MAC) with respect to the initial baseline model, the following inequality constraints can be included in the definition of Eqs. (22b):

$$\mathbf{c} = (\dots, \text{MAC}(\boldsymbol{\phi}_i^0, \mathbf{z}_{\phi_i}) - \text{MAC}(\boldsymbol{\phi}_i, \mathbf{z}_{\phi_i}), \dots) \leq \mathbf{0}, \quad i = 1, N_M, \quad (24)$$

where $\boldsymbol{\phi}_i^0$ is the i th eigenvector computed on the initial model, \mathbf{z}_{ϕ_i} the corresponding measured eigenvector, and the operator $\text{MAC}(\cdot, \cdot)$ is defined as

$$\text{MAC}(\mathbf{a}, \mathbf{b}) = \frac{(\mathbf{a}^T \mathbf{b})^2}{(\mathbf{a}^T \mathbf{a})(\mathbf{b}^T \mathbf{b})}. \quad (25)$$

2.4 Definition of model parameters

Wind turbine blades, being realized using composite materials and designed under a number of aero-elastic and manufacturing constraints, often present complex distributions of the stiffness, mass and inertial properties along their spans. More often than not, the property distributions present jump discontinuities, for example in correspondence of the beginning and ending of shear-webs, or very high gradients.

In order to accurately represent such complex property distributions, beam analysis codes for wind turbine applications typically define a large number of sectional properties along the blade span. The direct use of such sectional properties as unknown parameters in the model update processes described above is impractical for a number of reasons. First, a large number of sections would imply a large number of unknown parameters, which in turn would imply a large computational cost. Second, and more importantly, the use of a large number of unknowns to represent beam properties along the span will decrease the observability of the problem.

To address these problems, the identification parameters \mathbf{p} of problem (18) are here defined in terms of interpolated multiplicative shape functions that deform a given baseline property distributions, as detailed next.

First, so as to account for possible discontinuities in the blade property distributions, the blade span is divided into N_{segm} segments, the k th segment being defined for $s_k \leq s \leq s_{k+1}$, where the values $0 = s_1, s_2, \dots, s_{N_{\text{segm}}+1} = L$ identify segment boundaries.

Next, the i th property at station s along the span of the updated model, noted $\pi_i(s)$, is expressed as

$$\pi_i(s) = \alpha_i(s) \pi_i^0(s), \quad (26)$$

where $\pi_i^0(s)$ is the value of the i th property for the initial model, while $\alpha_i(s)$ are the computed scaling factor with respect to those values. The number of identified properties is noted N_{prop} , and $\pi_i(s)$ can represent any one of the parameters of the beam model, as for example mass per unit span, sectional inertias, bending, torsional, axial and shear (according to the assumptions of the model) stiffnesses. For s in the k th segment, i.e. $s \in [s_k, s_{k+1}]$, the scaling parameters are defined as

$$\alpha_i(s) = \sum_{j=1}^{N_{\text{nodes}}^k} n_j(\xi) \alpha_{i_j}^k, \quad (27)$$

where $n_j(\xi)$ are shape functions expressed in terms of the non-dimensional abscissa $\xi \in [0, 1]$,

$$\xi = \frac{s - s_k}{s_{k+1} - s_k}, \quad (28)$$

and $\alpha_{i_j}^k$ are the associated N_{nodes}^k nodal values for segment k .

Finally, the optimization parameters are defined as the nodal values of the shape function, i.e.

$$\mathbf{p} = (\dots, \alpha_{i_j}^k, \dots)^T, \quad i = 1, N_{\text{prop}}, \quad j = 1, N_{\text{nodes}}^k, \quad k = 1, N_{\text{segm}}. \quad (29)$$

3 Results

3.1 Preliminary study using simulated data

At first, we consider the application of the proposed procedures to a simulation case, with the goal of verifying the well-posedness of the problem and the identifiability of the unknown parameters.

To this aim, we consider the 61.5 meter long wind turbine blade of Ref. [12]. For simplicity of this preliminary study, the identification parameters were chosen as constants defined on three segments of equal length, as shown in Fig. 1, for each structural property (i.e. flap-wise, edge-wise and torsional stiffnesses, and mass per unit span).

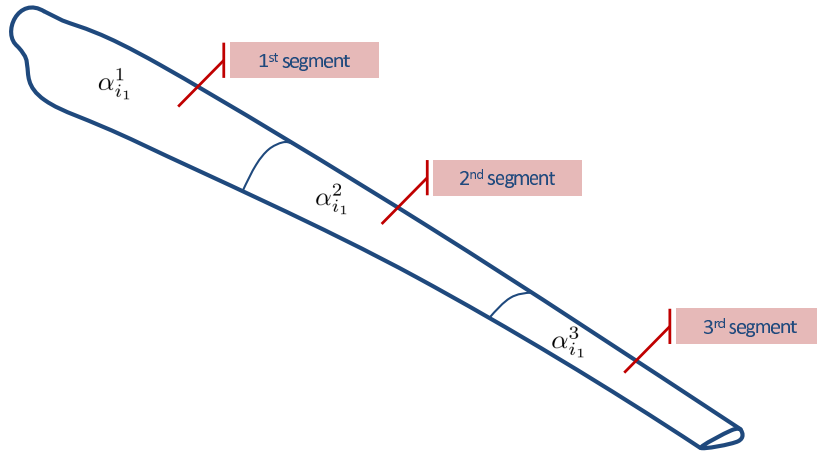


Fig. 1: Definition of identification parameters for the preliminary simulation study.

The blade, clamped at the root and subjected to gravity, was loaded first with a tip force in the flap-wise direction, then in the edge-wise direction, and finally with a tip torsional moment. The outputs included the displacements and rotations of ten uniformly spaced sections along the blade span, as well as the lowest five modal frequencies. All measures were added to a zero-mean gaussian white error with standard deviation equal to the 0.5% of their maximum value.

Eigenvectors were not included in this simulated example, for two reasons. First, in actual laboratory experiments eigenvectors are more difficult to measure than eigenvalues and they are often associated with higher levels of noise and uncertainty [2]. Second, eigenvectors often carry a smaller informational content than eigenvalues; this can be explained, for example, by recalling that the modal shapes of a beam of constant properties do not depend on the beam properties but only on the boundary conditions. This fact was confirmed by numerical experiments, which showed that the use of eigenvectors brings little benefit to the quality of the property estimates of wind turbine blades that are obtained by the sole use of eigenvalues and static deflections.

To ease convergence and robustify the procedure, the identification was conducted using a divide and conquer approach, that exploits the fact that the change of each set of properties (flap-wise, edge-wise, torsional stiffness and mass) has a predominant effect only on some of the

outputs. For example, flap-wise displacements have a high informational content regarding flap-wise stiffness, a small (although not null, due to blade twist) informational content on edge-wise stiffness, and an even smaller content on the torsional one. This suggests to divide the set of optimization parameters into several groups, and to perform the identification for each group separately using only the outputs that carry the highest informational content. Notice that, since in reality all parameters have some influence on all outputs, although small in some cases, the process must be iterated until convergence in order to correctly capture all couplings.

The procedure, used here and in the following, can be summarized as follows:

1. Estimate flap-wise, edge-wise and torsional stiffnesses, one at a time, keeping the other ones frozen at their last updated values, using static test deflections.
2. Maintaining the blade stiffness properties fixed, estimate the mass distribution using only modal information, while enforcing constraints on measured total mass and center of gravity position, as well as MAC constraints if mode shapes are available.
3. Return to step 1. and repeat until convergence.

Table 1 summarizes the results of this identification exercise using simulated data. The results show that flap-wise stiffness is more precisely identifiable than edge-wise stiffness, which in turn is more precisely identifiable than torsional stiffness. This can be explained by the fact that the three stiffnesses have decreasing (in the order flap, lag and torsion) effects on the response of the blade, as expected. Likewise, the properties associated with the central part of the blade are more precisely identifiable than the ones towards the root, which in turn are more precisely identifiable than the ones of the tip region. This is due to the fact that the central part of a wind turbine blade is usually the one that contributes the most to the rigidity of the structure.

Parameters		Real	Initial	Identified
Flap-wise	α_{11}^1 (root)	1.0	1.2	1.011
	α_{11}^2 (central)	1.0	1.2	1.001
	α_{11}^3 (tip)	1.0	1.2	1.011
Edge-wise	α_{21}^1 (root)	1.0	0.8	0.996
	α_{21}^2 (central)	1.0	0.8	0.997
	α_{21}^3 (tip)	1.0	0.8	1.007
Torsional	α_{31}^1 (root)	1.0	0.9	1.002
	α_{31}^2 (central)	1.0	0.9	0.994
	α_{31}^3 (tip)	1.0	0.9	0.991
Mass	α_{41}^1 (root)	1.0	1.1	1.013
	α_{41}^2 (central)	1.0	1.1	0.995
	α_{41}^3 (tip)	1.0	1.1	0.969

Tab. 1: Identified parameters for the preliminary study using simulated data.

3.2 Model update of wind turbine blades

Next, we consider the identification of the structural properties of two real wind turbine blades using experimental data, named in the following blades A and B, respectively.

3.2.1 Blade A

The blade was tested by a consultant of the manufacturer for the purpose of verifying the resistance of the blade. Although these tests were not designed for identifying the blade structural properties, it was found that the collected data was of sufficient quality and informational content even for this purpose, although with the limitations and problems noted here below.

The blade, of 6.2 meters of length, was weighted multiple times, by suspending it at different span-wise locations using two cables equipped with load cells. The total mass and span-wise location of the center of gravity along the blade pitch axis were obtained as the mean values of those computed from each one of the weighting trials.

In order to perform the static tests, the blade was bolted at the root and equipped with five saddles placed along its span. Loads were applied at each saddle in the vertical direction at three different points labeled C_0 , C_1 and C_2 , as shown in Fig. 2, via cables equipped with load cells and connected to an overhead traveling crane. Wire distance transducers were attached at points A_1 and A_2 on each saddle, as shown in Fig. 2; an additional wire transducer was attached at the blade tip.

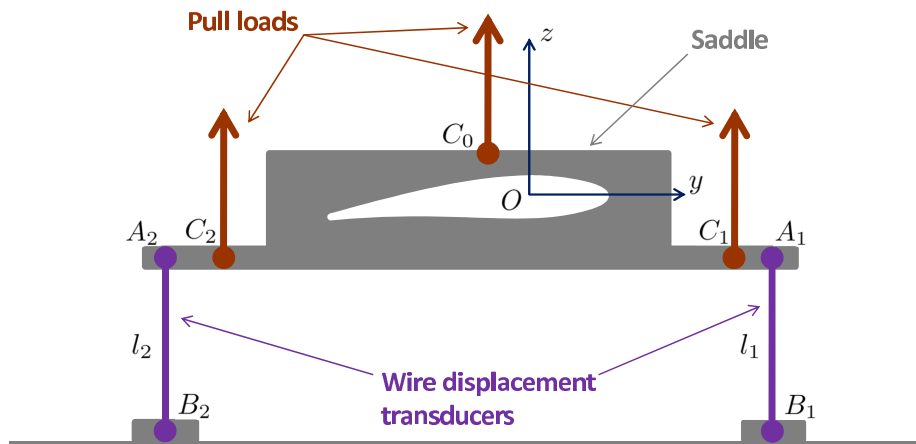


Fig. 2: Sketch of saddle used for the loading of blade A.

From the measures provided by the wire transducers, the vertical deflections δ_s and the torsional rotations δ_r of each sections were obtained under the assumption of small deviations from the reference configuration, which holds in the case of the present measurements.

The lowest modal frequencies of the blade were estimated by installing two orthogonal mono-axial accelerometers at a span-wise distance of 4510 mm from the root, and impacting the blade using a shock hammer.

The blade was subjected to various loads inducing either mostly flap-wise or mostly torsional deformations. For the flap-wise tests, for each load case only one saddle was loaded at point C_0 . Similarly, for the torsional tests, for each load case only one saddle was loaded at point C_1 so as to induce torsional rotations. Notice that some of these load cases are far from optimal from the point of view of the identification of blade structural properties. In fact, whenever outboard saddles

are unloaded, a complete section of the blade behaves as a rigid body. Therefore, displacement measures along it carry no informational content on its stiffness characteristics. Furthermore, only few measurements were made, and this prevented us from reserving a part of the data set for the validation of the identified model, as commonly done.

The lack of tests with edge-wise loading did not allow for an accurate estimation of the edge-wise stiffness distribution. To correct for this deficiency in the data, we resorted to the following procedure:

1. Estimate flap-wise stiffness distribution using flap-wise static loading experiments.
2. Estimate torsional rigidity distribution using torsional static loading experiments.
3. Estimate mass distribution using first and second flap-wise modes, with total mass and center of gravity position as constraints.
4. Estimate edge-wise stiffness distribution using first and second edge-wise modes. Note that, using only two measures, at most two parameters can be identified.
5. Return to step 1. and repeat until convergence.

For some of the loading conditions, Fig. 3 shows the measured deflections (triangular symbols), the deflections computed with the model prior to identification (dashed lines), and the ones after identification (solid lines), plotted as a function of the non-dimensional blade span $\eta = s/L$. Table 2 reports the measured eigenfrequencies, as well as the ones prior to and after identification. For all outputs, the initial large discrepancies are markedly reduced after identification, and the identified model appears to be well correlated with the experimental data.

Mode	I Flap	I Edge	II Flap	II Lag
Initial model	3.79	6.94	12.72	22.86
Identified model	3.59	7.48	11.88	25.22
Measures	3.65	7.43	10.89	27.34

Tab. 2: Lowest natural frequencies of blade A.

The estimated blade properties are displayed in Fig. 4. Each figure shows the initial (dashed lines) and the identified (solid lines) properties, as well as their Cramér-Rao standard deviations. Because a nominal torsional rigidity was not available prior to identification, Fig. 4(c) shows only the identified one. Notice that the edge-wise stiffness and mass distributions have a lower level of confidence than the other quantities; this is due to the lack of specific edge-wise loading conditions, as noted above.

3.2.2 Blade B

A second, different, wind turbine blade was tested by its manufacturer; these tests were specifically aimed at supporting a model update activity.

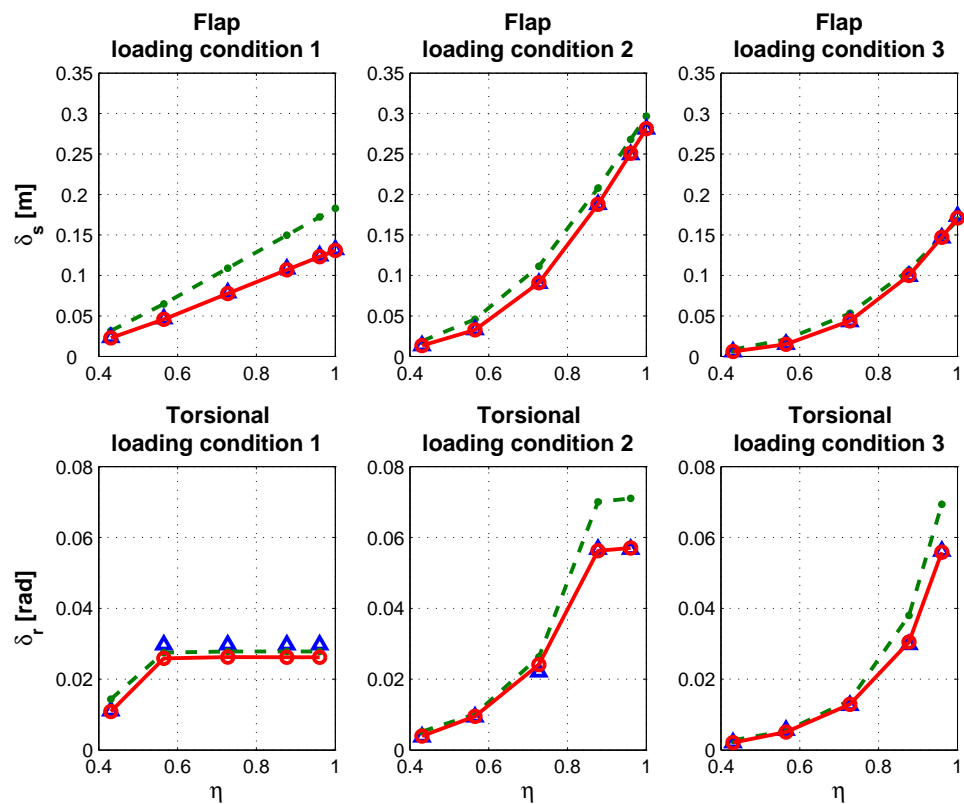


Fig. 3: Static deflections for some loading conditions of blade A. Triangle symbols: experimental data; dashed lines: initial model; solid lines: identified model.

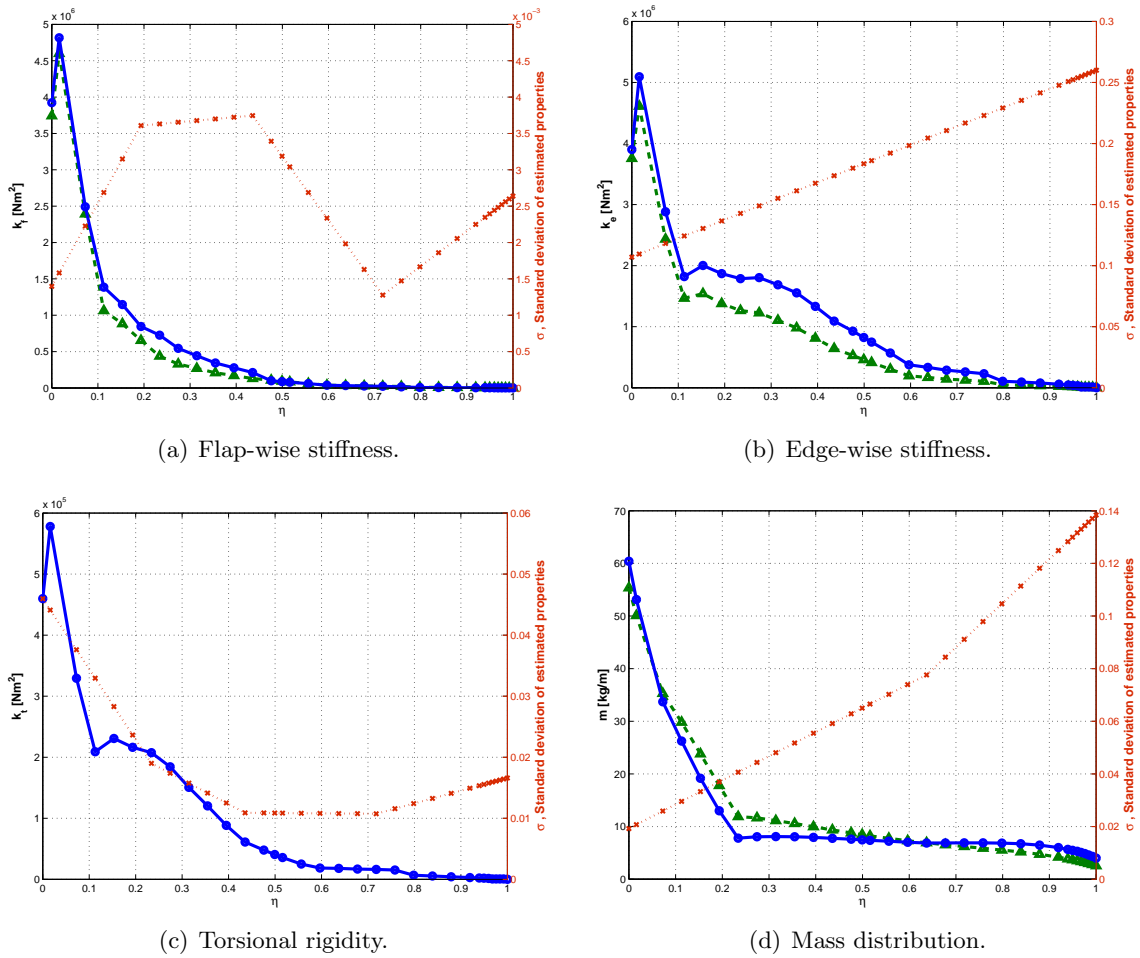


Fig. 4: Blade A: span-wise distribution of initial (dashed lines) and identified (solid lines) properties, and their Cramér-Rao standard deviations (dotted lines).

The blade, of 7.52 meters of length, was weighted multiple times by suspending it at different span-wise locations using two cables equipped with load cells, in order to compute its total mass and center of gravity location.

The blade was bolted at the root and equipped with three saddles placed along its span. Loads were applied at each saddle in a direction making an angle α with respect to the vertical, at two different points labeled C_0 and C_1 (cf. Fig. 5), via a cable equipped with a load cell connected by means of snap hooks.

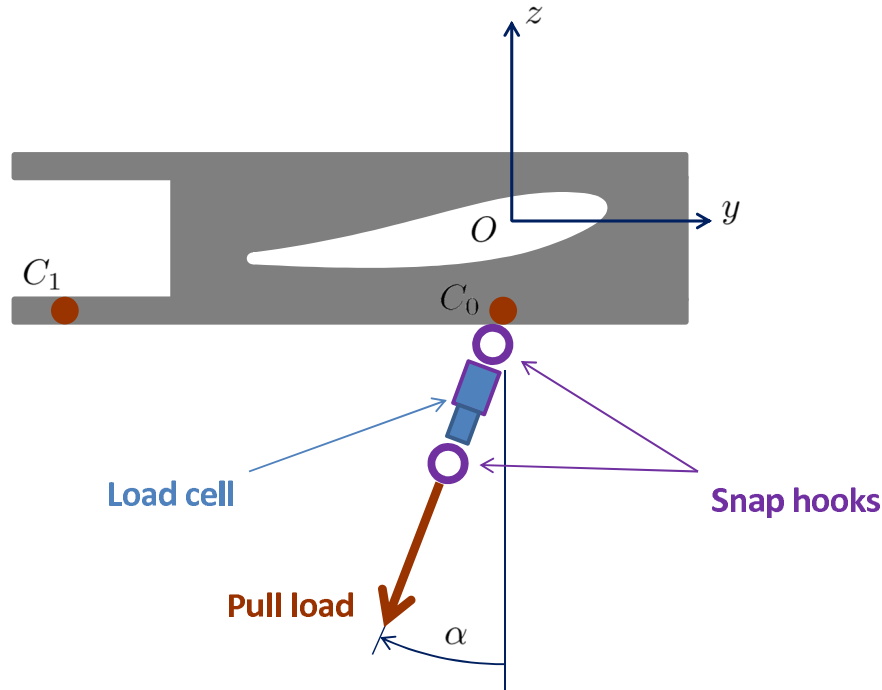


Fig. 5: Sketch of saddle used for the loading of blade B.

Separate load conditions involving mainly flap-wise, mainly edge-wise and mainly torsional responses were considered. For each condition (mainly flap, edge or torsional), three different cases were considered, of which two were used for conducting the identification, while the third one was used for the validation of the estimated model parameters. For the first load condition all three saddles were loaded, while for the second condition only the two saddles closer to the tip were loaded; finally, for the third condition loads were applied only at the tip saddle. Such conditions are linearly independent, so that the use of one of them for validation after identification constitutes a meaningful verification of the goodness and generality of the identified model.

Load magnitudes were chosen not to exceed maximum allowed ones, but also large enough to excite not too small a response, given the fact that the present blade is short and rather stiff.

The deflection of the blade was measured using a **Leica Scan Station C10** laser scanner [13]. Black markers were placed on the blade surface at nineteen equally spaced sections along the blade span. Scan data was processed with the **Leica Cyclone 7.1** software, that allows one to obtain the marker coordinates in a given reference frame. Measurements were also performed on the unloaded blade, so as to obtain the deflected configuration under the action of the sole

gravitational field. Figure 6 shows some typical blade scan images obtained during the laboratory experiments.

Once computed the marker coordinates using the laser scanner software, the motion of each blade section was obtained by a non-linear least squares fit. With reference to Fig. 7, the blade pitch axis is located at point H in the unloaded configuration, and at point K in the loaded one; similarly, the m th marker is located at P_m in the unloaded case, and at Q_m in the loaded one. The relationship between the two configurations can be written as

$$(Q_m - H) = \mathbf{T}(P_m - H) + \mathbf{s}, \quad (30)$$

where \mathbf{s} is the unknown sectional translation vector, and $\mathbf{T}(\boldsymbol{\psi})$ the rotation tensor parameterized in terms of the unknown rotation vector $\boldsymbol{\psi} = \varphi \mathbf{k}$, with rotation angle φ and rotation axis \mathbf{k} . Finally, the sectional motion is computed as

$$\{\mathbf{s}, \boldsymbol{\psi}\} = \arg \min_{\mathbf{s}, \boldsymbol{\psi}} \sum_{m=1}^{N_{\text{mark}}} ((Q_m - H) - \mathbf{T}(P_m - H) + \mathbf{s})^2, \quad (31)$$

where N_{mark} is the number of markers for the considered blade section.

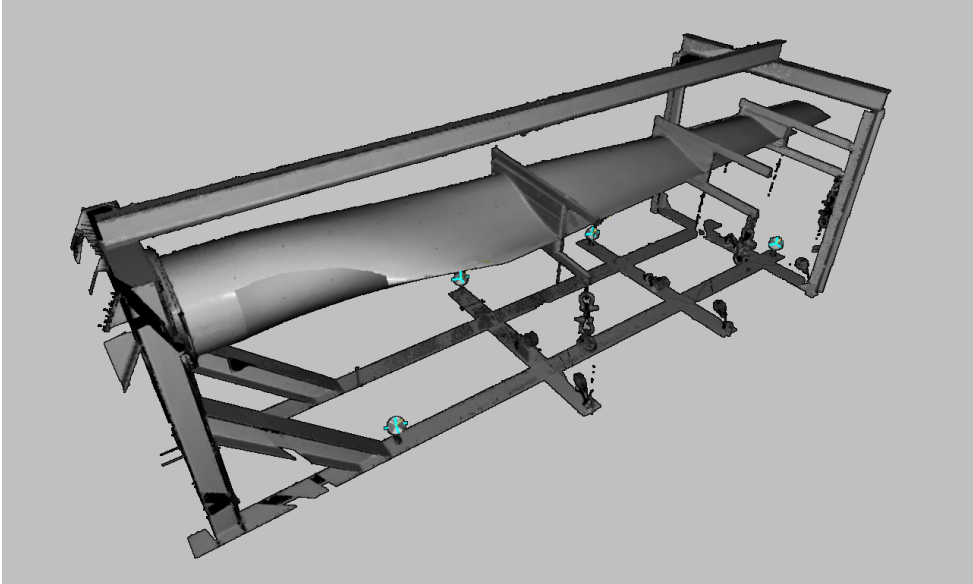
The lowest modal frequencies of the blade were estimated by installing fifteen mono-axial accelerometers along the blade span and impacting the blade using a shock hammer. Figure 8 shows the FFT for accelerometers #1, #2 and #3 (i.e. those at the blade tip) as well as #15 (placed at the root bolted connection, on the frame side), for excitations in the flap-wise (at left) and edge-wise (at right) directions. The shock hammer tests were repeated twenty times, and the first four blade natural frequencies, computed as the mean values of all trials, were used as modal outputs in the identification process.

It appears that the root constraint is not perfectly rigid, and in fact the supporting frame is subjected to vibrations as indicated by accelerometer #15; the flexibility of the frame will be further confirmed by the static test measures (see Fig. 9 later on). This will be taken into account during the estimation of the blade model parameters, by introducing unknown stiffnesses at the root boundary condition so as to model this effect.

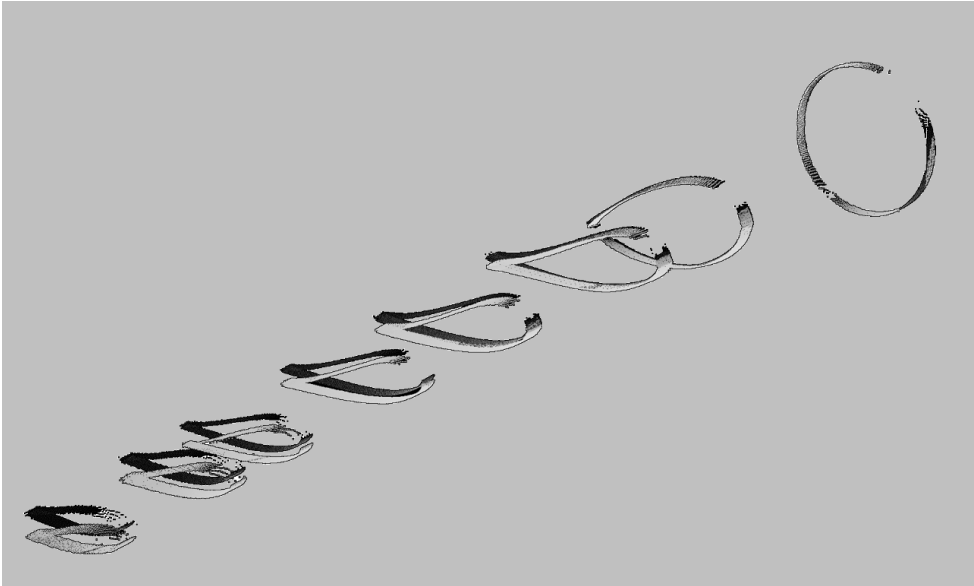
All nominal blade properties showed a marked discontinuity at the 4% span location, due to a change in the lamination sequence in the root region. Accounting for this, the identification parameters were also allowed to jump at that location by using two segments (see definition of model parameters in §2.4). The root segment was associated with a single (span-wise) constant identification unknown; the same constant was used in the flap-wise and edge-wise directions, to account for the cylindrical shape of the blade at the root. For the rest of the blade we used piecewise linear shape functions, whose free parameters were determined by performing the identification for an increasing number of them until satisfactory results were obtained.

In order to model the flexibility of the supporting frame of the blade, three (flap-wise, edge-wise and torsional) springs of unknown stiffness were added to the blade model at the root clamp, and included in the set of identification parameters. It was observed that the addition of these unknowns rendered the problem harder to solve, since they tended to produce effects on the outputs that were highly correlated with the ones due to the parameters modeling the blade root region. A detailed study of the Fisher information matrix showed that the couple of spring/root parameters related to the edge-wise stiffnesses had a better level of identifiability than the flap-wise pair.

This fact was exploited in the divide and conquer iterative identification as follows. At first we estimated the edge-wise stiffness distribution and edge-wise root spring using edge-wise static



(a) Scanner image of a torsional static test.



(b) Unloaded (dark) and loaded (light) blade cross sections, for one of the torsional loading conditions.

Fig. 6: Laser scanner images of blade and supporting frame.

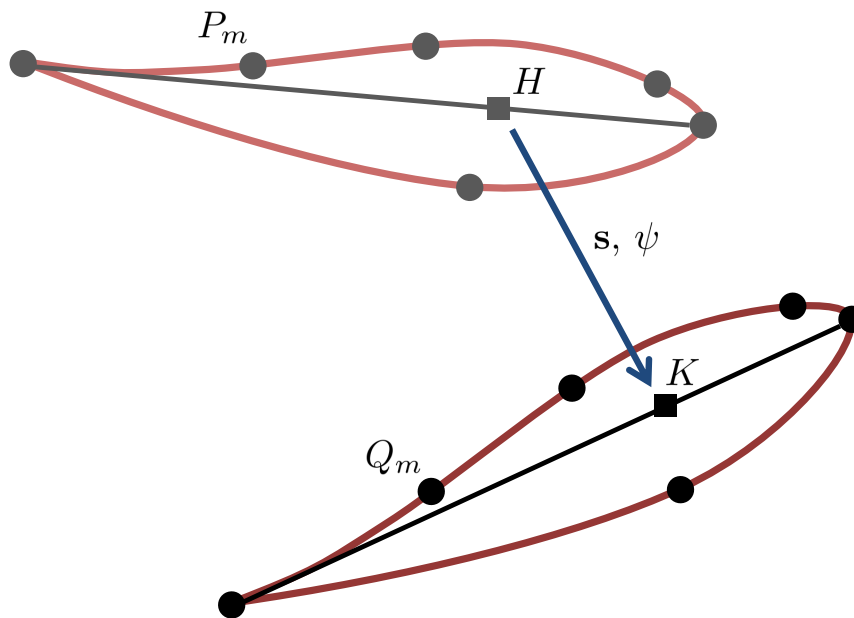


Fig. 7: Computation of translation and rotation of a blade section from its marker coordinates.

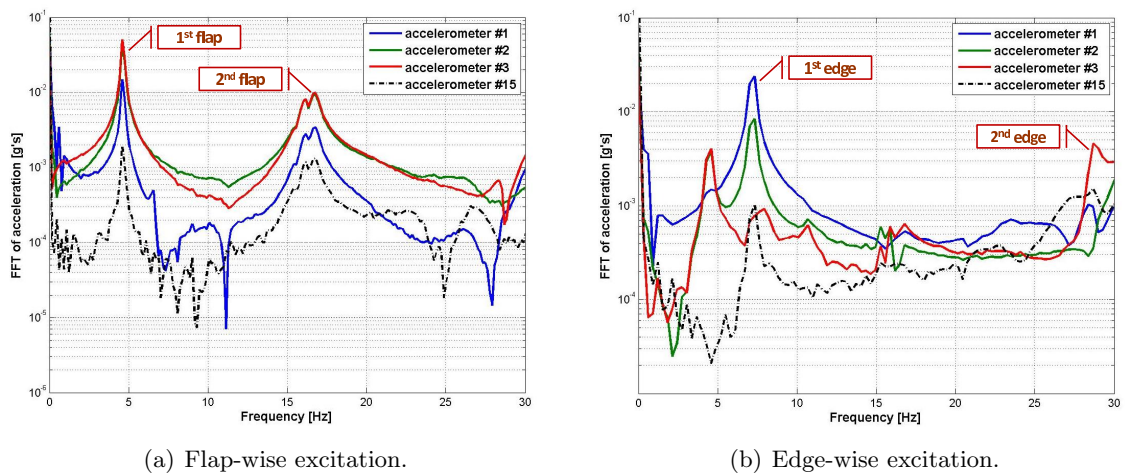


Fig. 8: FFT of some blade accelerometers for shock hammer tests.

load experiments. Next, we estimated the flap-wise stiffness distribution and flap-wise root spring using flap-wise static load experiments; in this step the blade root parameter was kept fixed at the value identified previously, thanks to the symmetry of the root region in the flap-wise and edge-wise directions. The procedure was then continued as already explained by considering torsional and modal tests, and iterated until convergence.

For all the loading conditions, Fig. 9 shows the measured deflections (triangular symbols), the deflections computed with the model prior to identification (dashed lines), and the ones after identification (solid lines); measured torsional rotations of the blade sections appear to be quite noisier than displacements. The rightmost column, labeled loading conditions 3, shows validation results, in the sense that the data was not used for the identification of the blade properties. All plots, including the validation ones, show a good quality of the identified model.

Notice, as mentioned previously, the flexibility of the supporting frame: in fact, the slopes of the measured deflections at the blade root ($\eta = 0$) are clearly different from zero, indicating a flexible root boundary condition.

Table 3 reports the measured eigenfrequencies, as well as the ones prior to and after identification.

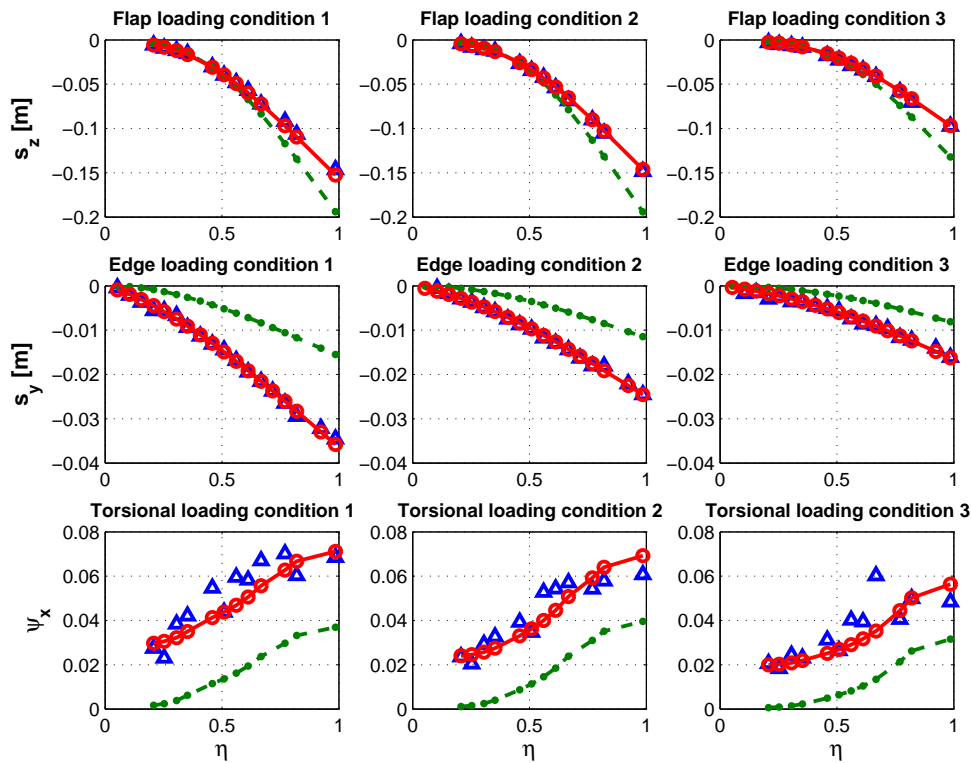


Fig. 9: Static deflections for the loading conditions of blade B. Triangle symbols: experimental data; dashed lines: initial model; solid lines: identified model. The rightmost column shows validation data, and was not used in the identification process.

The estimated blade properties are displayed in Fig. 10. Each figure shows the initial (dashed lines) and the identified (solid lines) properties, as well as their Cramér-Rao standard deviations. Notice the very large discrepancy between the nominal and identified mass properties; for unknown reasons the former were affected by large errors, as also readily shown by the initial weighting of the blade.

Mode	I Flap	I Edge	II Flap	II Lag
Initial model	4.677	8.994	18.71	39.56
Identified model	4.579	6.876	16.06	29.51
Measures	4.578	7.172	16.78	28.69

Tab. 3: Lowest natural frequencies of blade B.

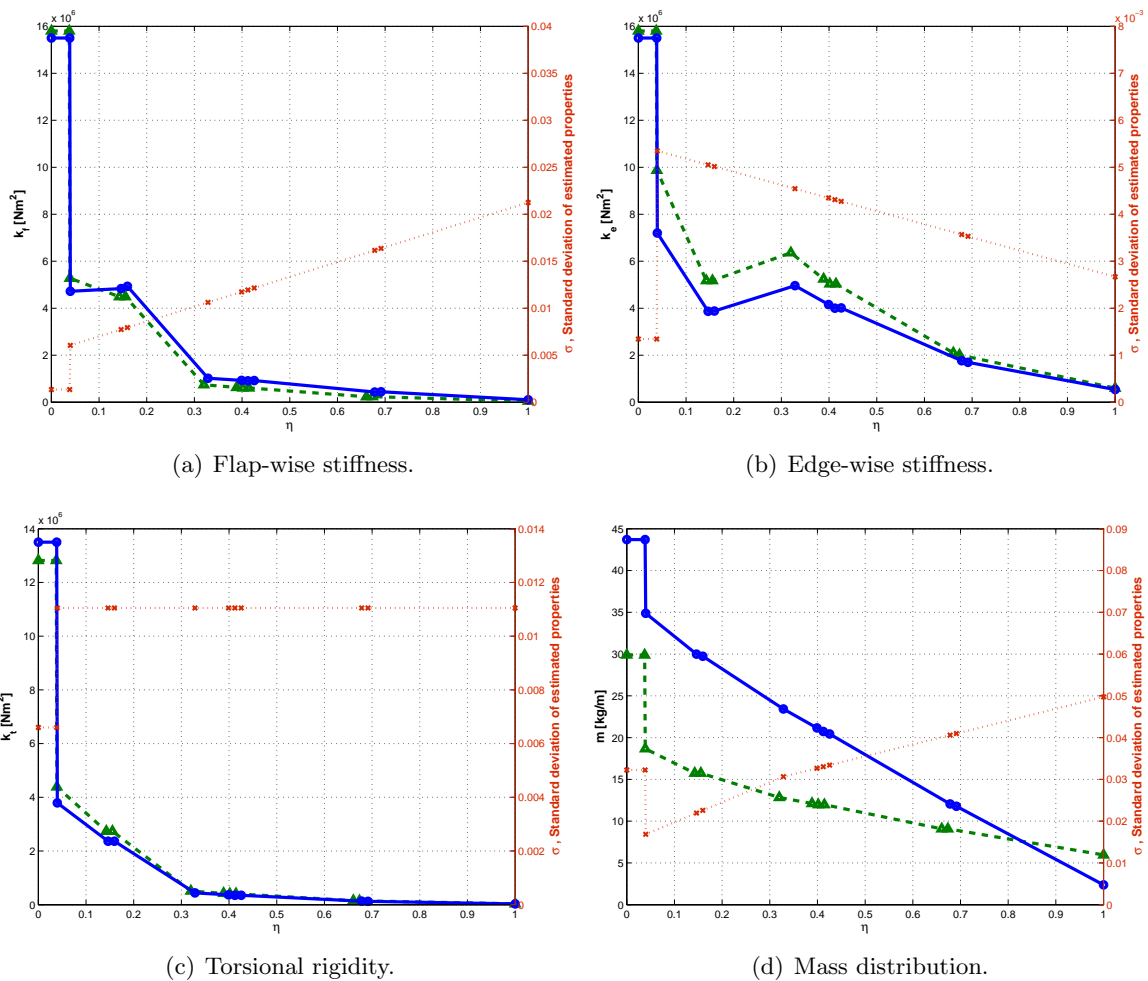


Fig. 10: Blade B: span-wise distribution of initial (dashed lines) and identified (solid lines) properties, and their Cramér-Rao standard deviations (dotted lines).

4 Conclusions

In this work we have presented a numerical procedure for the estimation of blade structural properties from experimental data. The proposed procedures can be used for identifying beam models of wind turbines, so as to improve the predictive capabilities of aero-elastic simulations. Furthermore, the same procedures can be used for understanding the nature of discrepancies between nominal design characteristics of the blade and the manufactured item, which in turn may have positive feedbacks which include improvements in the manufacturing process and better characterization of material properties.

The proposed procedures were tested with the help of simulated and real experimental data. From the presented results, as well as extensive testing with other blade identification problems not reported here for brevity, the following conclusions can be drawn:

- Using multiple experiments in a measurement fusion approach, as the one pursued here, improves the quality of the estimates; specifically, we found that the use of static load tests can lead to better estimates of the blade structural parameters than those obtained by the sole use of measured natural frequencies.
- The inclusion of equality and inequality constraints is an effective way of including all available information in the estimation problem. The use of bounds on the estimation parameters can help in assuring that the results are within physically admissible limits.
- As for all parameter estimation problems, great care has to be taken to ensure the well posedness of the problem, and the identifiability of unknown parameters. This issue was considered here by studying the Fisher information matrix.
- The use of a divide and conquer approach can greatly robustify the procedure. By breaking the identification parameters into groups, one can use the measures that carry the highest informational content for each specific group, and this leads to smaller and better conditioned problems. All couplings among the various groups can be recovered by iteratively repeating the sub-identification problems for each group. Such iterations were found to converge very quickly.
- The adaptive estimation of the error covariance leads to an iterative solution of least-squares-like problems with given weighting. The maximum likelihood formulation relieves the user from the choice of the weighting factors, which are computed automatically. This proved to be useful especially when considering multiple diverse measurements, as in the present case.
- Experiments aimed at providing data for parameter estimation should be carefully designed so as to provide complete results with a sufficient level of accuracy. Incomplete load cases, imperfect clamp conditions, partial recording of blade section motions and other limitations were found here to complicate the identification process of the tested blades.
- The use of gradient-based methods, SQP in the present case, leads to relatively fast execution times, high precision solutions and an exact handling of linear and non-linear constraints. On the other hand, one can not guarantee the achievement of the global optimum, and trapping in local minima is possible. The use of global optimizers, possibly coupled to the present local one for efficiency, should be pursued in the continuation of this research.

Acknowledgements

This work is supported by the Alliance for Sustainable Energy LLC, National Renewable Energy Laboratory (NREL), sub-contract No. AFC-1-11301-01, technical monitors Dr. Gunjit Bir and Alan Wright. The authors acknowledge Tozzi Nord S.r.l. and CRIEL S.r.l. for providing the blade data. L.C. Henriksen, A. Sacchetti and A. Trimarco have contributed in the development and testing of the computational procedures described in this document.

References

- [1] M. Morandini, M. Chierichetti and P. Mantegazza, Characteristic Behavior of Prismatic Anisotropic Beam via Generalized Eigenvectors, *International Journal of Solids and Structures*, **47**, 1327–1337, 2010.
- [2] M.I. Friswell and J.E. Mottershead, *Finite Element Model Updating in Structural Dynamics*, Kluwer Academic Publishers, 1995.
- [3] R.V. Jategaonkar, *Flight Vehicle System Identification: a Time Domain Methodology*, AIAA, Progress in Astronautics and Aeronautics, Vol. 216, Reston, VA, USA, 2006.
- [4] V. Klein and E.A. Morelli, *Aircraft System Identification: Theory and Practice*, AIAA, Education Series, Reston, VA, USA, 2006.
- [5] G. Kerschen, K. Worden, A.F. Vakakis and J.C. Golinval, Past, Present and Future of Nonlinear System Identification in Structural Dynamics, *Mechanical Systems and Signal Processing*, **20**, 505–592, 2006.
- [6] A. Barclay, P.E. Gill and J.B. Rosen, SQP Methods and their Application to Numerical Optimal Control, Report NA 97–3, Department of Mathematics, University of California, San Diego, CA, 1997.
- [7] K. Christodoulou, E. Ntotsios, C. Papadimitriou and P. Panetsos, Structural Model Updating and Prediction Variability using Pareto Optimal Models, *Computer Methods in Applied Mechanics and Engineering*, **198**, 138–149, 2008.
- [8] Y. Haralampidis, C. Papadimitriou and M. Pavlidou, Multi-Objective Framework for Structural Model Identification, *Earthquake Engineering and Structural Dynamics*, **34**, 665–685, 2005.
- [9] S.V. Modak, T.K. Kundra and B.C. Nakra, Model Updating using Constrained Optimization, *Mechanics Research Communications*, **27-5**, 543–55, 2000.
- [10] J. Renegar, *A Mathematical View of Interior Point Methods in Convex Optimization*, SIAM, Philadelphia, 2001.
- [11] R.B. Nelson, Simplified Calculation of Eigenvector Derivatives, *AIAA Journal*, **14**, 1201–1205, 1976.
- [12] J. Jonkman, S. Butterfield, W. Musial and G. Scott, Definition of a 5-MW Reference Wind Turbine for Offshore System Development, NREL/TP-500-38060, National Renewable Energy Laboratory, Golden, CO, USA, 2007.

-
- [13] Leica Geosystems AG, Heinrich Wild Strasse. CH-9435 Heerbrugg, St. Gallen, Switzerland,
<http://www.leica-geosystems.com/>.